"REVISED II"

Effect of Mixed γand χ Crystalline Phases in Nanocrystalline Al_2O_3 on the Dispersion of Cobalt on Al_2O_3

Kamonchanok Pansanga[a], Joongjai Panpranot[a], Okorn Mekasuwandumrong[b], Chairit Satayaprasert[a], James G. Goodwin, Jr.[c], and Piyasan Praserthdam[*,a]

[a] Center of Excellence on Catalysis and Catalytic Reaction Engineering, Department of Chemical Engineering, Faculty of Engineering, Chulalongkorn University, Bangkok 10330, Thailand

[b] Department of Chemical Engineering, Faculty of Engineering and Industrial Technology, Silpakorn University, Nakorn Pathom 73000, Thailand

[c] Department of Chemical and Biomolecular Engineering, Clemson University, Clemson, South Carolina, 29634, USA

Keywords: nanocrystalline alumina; crystalline phase; cobalt catalyst; CO hydrogenation; χ alumina; γalumina

Submitted to: *Catalysis Communications*

Date: May 22, 2007

[*] All correspondence should be addressed.

Tel: 66-2218-2882 Fax: 66-2218-6877 E-mail: piyasan.p@chula.ac.th

Abstract

This paper reports the results of a study into the effect of mixed γ and χ crystalline phases in Al_2O_3 on the characteristics and catalytic activities for CO hydrogenation of Co/Al_2O_3 catalysts. The catalysts were characterized by X-ray diffraction, N_2 physisorption, transmission electron microscopy, and H_2 chemisorption. Increasing Co loading from 5 to 20 wt% for the mixed phase Al_2O_3-supported Co catalysts resulted in a constant increase in both the number of cobalt metal active sites and the hydrogenation activities. However, for those supported on γ-Al_2O_3, Co dispersion increased up to 15 wt% Co and declined at 20 wt% Co loading. It is suggested that the spherical-shape like morphology of the χphase Al_2O_3 prevented agglomeration of Co particles, especially at high Co loadings.

1. Introduction

Alumina is one of the most common commercial carriers used to disperse catalytic materials because of its excellent thermal stability, high mechanical resistance, and wide range of chemical, physical, and catalytic properties. In general, acidic, high surface area alumina hydrates are produced at relatively low temperatures by precipitation from either acidic or basic solutions and then are transformed to "transition" β, γ, η, χ, κ, δ, θ, and αAl_2O_3 by dehydration and treatment at high temperatures [1].

Despite a wide range of crystalline structures, only γ- and αAl_2O_3 have been studied often as catalyst supports. Typically, γ-Al_2O_3 provides a better dispersion of catalytically active metals than αAl_2O_3 due to its higher surface area. Only a few publications have reported the effect of other crystalline phases of alumina on the properties of alumina-supported catalysts. For example, Chary et al. [2] reported that dispersion of vanadium oxide on alumina as well as its catalytic activities in partial oxidation decreased with increasing calcination temperature due to the transformation of γ-alumina into θ-alumina, δ-alumina, and α-alumina phases. Recently, Moya et al. [3] studied silver nanoparticles supported on α, η, and δ-Al_2O_3 prepared by a colloidal processing route. It was found that silver particle sizes varied between 1-100 nm depending on the alumina phase. To our knowledge, the effect of mixed γ- and χ-Al_2O_3 phases on the properties of Al_2O_3 as a catalyst support has never been reported.

In this study, nanocrystalline transition Al_2O_3 (γ-Al_2O_3 and mixed γ- and χ-Al_2O_3) were synthesized by decomposition of aluminum isopropoxide (AIP) under solvothermal conditions. The advantages of the solvothermal method are that it gives products with uniform morphology, well-controlled chemical composition, and

narrow particle size distribution [4-8]. Furthermore, desired shapes and sizes of particles can be tailored by controlling process conditions such as solute concentration, reaction temperature, reaction time, and the type of solvent [9-10]. The effects of mixed crystalline phases of Al_2O_3 on the dispersion of cobalt on Al_2O_3 and the resulting catalytic activity for CO hydrogenation were investigated.

2. Experimental

2.1. Preparation of alumina

Nanocrystalline transition Al_2O_3 was prepared by the solvothermal method according to the procedure described in Ref. [11]. The desired amount of aluminum isopropoxide (AIP) (Aldrich) (10, 15, 25, or 35 g) was suspended in 100 ml of 1-butanol (Ajax Finechem) in a beaker, which was then placed in a 300 ml autoclave. In the gap between the beaker and the autoclave wall, 30 ml of 1-butanol was added. After the atmosphere inside the autoclave was purged completely with nitrogen, the mixture was heated to 300°C at a heating rate of 2.5°C/min and was kept at that temperature for 2 h. After cooling to room temperature, the resulting powders were collected after repeated washing with acetone and were then air-dried. The calcination of the products was carried out in a box furnace by heating up to 600°C at a rate of 10°C/min and held at that temperature for 1 h.

2.2. Catalyst preparation

The Al_2O_3-supported cobalt catalysts with different Co loadings (5, 10, 15, and 20 wt%) cobalt were prepared by incipient wetness impregnation of alumina with a desired amount of an aqueous solution of cobalt nitrate [$Co(NO_3)_2 \cdot 6H_2O$] (Aldrich).

After impregnation, the catalysts were dried at 110°C for 24 h and calcined in air at 300°C for 2 h using a ramp rate of 1°C/min.

2.3 Catalyst characterization

X-ray diffraction patterns of the samples were collected using a SIEMENS D-5000 X-ray diffractometer with Cu K_α radiation (λ = 1.54439 Å). The spectra were scanned at a rate of 0.04°/step from 2θ = 15° to 80°. The composition of each crystalline phase has been calculated from the calibration of X-ray diffraction peak areas of the mixtures between each pure phase (physically mixed). BET surface areas of the sample were calculated using the BET-single point method at liquid N_2 temperature. Transmission electron microscopy was performed to study the morphologies of the catalyst samples and the dispersion of cobalt oxide species on the alumina supports using a JEOL JEM 1230. The number of surface cobalt metal atoms was determined by pulse H_2 chemisorption at 100°C on the reduced cobalt catalysts based on the static method described by Reuel and Bartholomew [12] using a Micromeritics Pulse Chemisorb 2750 system. Prior to H_2 chemisorption, the catalyst samples were reduced at 350°C in flowing H_2 for 3 h. The X-ray photoelectron spectroscopy (XPS) analysis was performed using an AMICUS photoelectron spectrometer equipped with a Mg K_α X-ray as a primary excitation and a KRATOS VISION2 software. XPS elemental spectra were acquired with 0.1 eV energy step at a pass energy of 75 kV. The C 1s line was taken as an internal standard at 285.0 eV.

2.4 Reaction study

CO hydrogenation was carried out at 220°C and 1 atm total pressure in a fixed-bed quartz reactor under differential reaction conditions. The H_2/CO ratio used was 10/1. Typically, 0.1 g of the catalyst sample was reduced *in situ* in flowing H_2 (50 cc/min) at 350°C for 3 h prior to reaction. After the start up, samples were taken at 1-h intervals and analyzed by gas chromatography. Steady state was reached within 6 h in all cases.

3. Results and Discussion

In this study, nanocrystalline alumina powders were prepared by thermal decomposition of AIP in 1-butanol with various AIP content. XRD patterns of these alumina samples after calcination at 600°C for 1 h are shown in **Figure 1**. The XRD patterns of transition Al_2O_3 were observed at degree 2θ= 31°, 33°, 38°, 43°, 47.5°, and 68°. It was found that when lower amounts of AIP were used (10 and 15 g in 100 cm^3 of 1-butanol), only γ-Al_2O_3 was formed by calcination, as seen by the XRD characteristic peaks at 2θ = 33° according to the JCPDSs database. These γ-Al_2O_3 samples are denoted hereafter as Al-G1 and Al-G2, respectively. The XRD characteristic peak of χ-alumina was observed at 2θ = 42.5° for the supports prepared with higher amounts of AIP (25 and 35 g in 100 cm^3 1-butanol). The mixed γ- and χ-crystalline phase samples containing χ-phase of ca. 33% and 57% were denoted as Al-GC1 and Al-GC2, respectively. Pure χ-alumina prepared by reaction of AIP in toluene was used as the reference sample and denoted as Al-C. The intensity of χ-Al_2O_3 peaks became stronger with increasing amount of AIP content during

preparation, indicating that increasing AIP content during the solvothermal synthesis resulted in formation of alumina giving rise to mixed phases of γ-Al_2O_3 and χ-Al_2O_3 after calcination. The physical properties of the various Al_2O_3 samples are shown in **Table 1**. The BET surface area of the Al-GC2 (145 m^2/g) was found to be twice of that of Al-G1 (70 m^2/g). A similar trend was observed for the bulk density of the Al_2O_3 powders. The bulk density increased with increasing amount of AIP used during preparation (from 0.38 g/cm^3 to 0.54 g/cm^3). The BET surface areas also increased with increasing AIP concentration, probably as a result of morphology changing from a wrinkled sheet structure to small spherical particles (see **Figure 3)**. These results were confirmed by Al-C with highest BET surface area (180 m^2/g), highest bulk density (0.56 g/cm^3) and complete spherical particle morphologies. From results such as these, it has been proposed that for preparation with low AIP contents, boehmite is the main product resulting in γ-alumina after calcination at 600°C for 1 h. The morphology of the boehmite products obtained via the solvothermal reaction has been shown to be wrinkled sheets [13-14]. The precursor to spherical-shaped χ-Al_2O_3 was formed by direct decomposition of AIP in the solvent and appeared to increase with increasing AIP concentration.

Figure 2 shows the IR spectra of alumina supports after calcination at 600°C for 1 h. The IR peaks assigned to OH stretching were observed at around 3730 and broad peak between 3200 to 3600 cm^{-1}. According to Peri's model [15], the features at 3791, 3730, and 3678 cm^{-1} are assigned to surface isolated hydroxyl groups. The broader peak at 3589 cm^{-1} is due to the vibration of associated hydroxyl groups of aluminum oxide. The spectra which assigned to OH groups of all samples were nearly identical. Therefore, the amounts and nature of OH groups of all supports were essentially same.

The nanocrystalline γ-Al_2O_3 and mixed γ- and χ-Al_2O_3 were then employed as catalyst supports for Co catalysts. The Co/Al_2O_3 catalysts were prepared using the incipient wetness impregnation method with cobalt loadings of 5, 10, 15, and 20 wt% in order to investigate the effect of mixed crystalline phases of Al_2O_3 on the dispersion of Co and its catalytic activity for CO hydrogenation. The XRD patterns of the various Co/Al_2O_3 catalysts after calcination at 300°C were not significantly different from those of the Al_2O_3 supports (results not shown). No XRD characteristic peaks of Co_3O_4 and/or other Co compounds were detected for all the catalyst samples. This suggests that the crystallite size of cobalt oxide on Al_2O_3 was probably below the lower limit for XRD detectability (3-5 nm). Such results also indicate that cobalt oxide species were present in a highly dispersed form on these nanocrystalline Al_2O_3 even for cobalt loadings as high as 20 wt%.

The morphology and distribution of cobalt oxide particles on the Al_2O_3 supports were investigated by transmission electron microscopy (TEM). The typical TEM micrographs of 20 wt% of cobalt on alumina supports containing different compositions of γ and χ phases are shown in **Figure 3**. In all the TEM figures, the darker spots on the catalyst granules represent a high concentration of cobalt and its compounds while the lighter areas indicate the support with minimal or no cobalt present. It was found that the wrinkled sheets-like structure of γ-Al_2O_3 was maintained after impregnation and calcination for both 20Co/Al-G1 and 20Co/Al-G2 catalysts (Figure 2a and 2b). The mixed structure between spherical particles of χ-Al_2O_3 and wrinkled sheets of γ-Al_2O_3 were also observed for 20Co/Al-GC1 and 20Co/Al-GC2 samples (Figure 2c and 2d). However, cobalt oxide species appeared to be more

agglomerated on the γ-Al_2O_3 supports than on the mixed γ- and χ-ones as shown by the appearance of larger cobalt oxide particles/granules.

Static H_2 chemisorption on the reduced cobalt catalyst was used to determine the number of active surface cobalt metal atoms [16]. The H_2 chemisorption results for all the catalyst samples are reported in **Table 2**. The overall dispersion of reduced Co and crystal size of Co^0 in the catalyst samples based on the H_2 chemisorption results is also given. In order to distinguish the effect of mixed γ and χ crystalline phases of Al_2O_3 and the effect of BET surface area, we also report the H_2 chemisorption results in terms of the amount of H_2 chemisorption per total specific surface area of the catalyst (see **Figure 4**). For the Co/Al-G1 and Co/Al-G2 catalysts in which the Al_2O_3 contained only the γ phase, the number of active surface cobalt metal atoms per unit surface area increased with increasing Co loading up to 15 wt%. Further increase of the amount of Co loading to 20 wt% resulted in both a lower cobalt dispersion and fewer exposed surface cobalt metal atoms (**Table 2**), even taking into account BET surface area (**Figure 4**). This is typical for supported Co Fischer-Tropsch catalysts. Dispersion usually decreases with increasing Co loading beyond a certain point [17-21]. On the contrary, the amounts of H_2 chemisorption per unit surface area of the mixed γ and χ crystalline phases Al_2O_3 supported Co catalysts (Co/Al-GC1 and Co/Al-GC2) constantly increased with increasing Co loading from 5 to 20 wt% (**Table 2, Figure 4**). To study the effect of phase composition on active sites of Co catalyst, 15%Co/pure χ-alumina catalyst was characterized to compare with 15%Co deposited on pure γ-Al_2O_3 and mix phase supports. The amounts of H_2 chemisorption increased from 9.2 to 21.4 μmol/g catalyst as the χ phase contents increased from 0 to 57%. While the amounts of H_2 chemisorption of Co/pure χ-

alumina catalyst ranged around 16.8 μmol/g catalyst. It is suggested that the presence of χ phase in γ-Al_2O_3 may prevent agglomeration of Co particles especially at high Co loadings, resulting in the maintenance of high Co dispersion. Because of its surface sensitivity, XPS is used to identify the surface compositions of the catalysts as well as the interaction between Co and the alumina supports. The results are given in Table 3. It was found that the ratio of Al/O atomic concentration was slightly increased while that of Co/Al decreased with the presence of χphase in γ-Al_2O_3 suggesting higher dispersion of Co on the mixed phase Al_2O_3 supports. There was also a slight shift of Co 2p binding energy to higher values for the 15Co/Al-GC1 and 15Co/Al-GC2 catalysts compared to those supported on γ-Al_2O_3 (Al-G1 and Al-G2). Such results suggest stronger interaction between Co and the mixed phases γ- and χ-Al_2O_3.

CO hydrogenation was carried out in a fixed-bed quartz reactor under differential reaction conditions in order to determine the catalytic activity of the catalyst samples. The reaction results in terms of CO conversion, hydrogenation rate, and the turnover frequency (TOF) per exposed Co atom calculated using the hydrogen chemisorption data are given in **Table 4**. The catalytic activities increased with increasing Co loading in general (at least to 15 wt% Co). For a similar Co loading, Co catalysts supported on the mixed crystalline phases Al_2O_3 exhibited higher CO hydrogenation activities compared to those supported on the ones containing only γ phase Al_2O_3. The TOFs of the cobalt catalysts in which the Al_2O_3 support contained only the γ phase decreased with increasing Co loading, suggesting perhaps an underestimation of exposed Co metal atoms by H_2 chemisorption. However, the TOFs for the mixed crystalline phases Al_2O_3 did not significantly change regardless of cobalt loading percentage. The reaction results are in a good agreement with the

H_2 chemisorption results since CO hydrogenation is usually considered to be a structure insensitive reaction [22-26]. Thus, higher dispersion of Co yields higher hydrogenation activity.

4. Conclusions

Nanocrystalline γ-Al_2O_3 and mixed γ and χ-Al_2O_3 were obtained by decomposition of AIP in 1-butanol by varying the amounts of AIP used under the solvothermal conditions. For a similar Co loading, the presence of χphase in γ-Al_2O_3 support resulted in higher dispersion of Co as well as higher CO hydrogenation activities of the Co/Al_2O_3 catalysts. It is suggested that the spherical-shape like morphology of the χphase Al_2O_3 provide better stability of the Co particles, especially for those with high Co loadings.

Acknowledgments

The authors would like to thank the Thailand Research Fund (TRF) for the financial support of this project.

Table 1 Properties of the various nanocrystalline Al_2O_3 samples prepared by the reaction of AIP in 1-butanol at 300°C for 2 h.

Samples	Amounts of AIP (g)	Amounts of χ phase (%)	Surface area (m^2/g)[a]	Bulk density (g/cm^3)[a]	Morphology [27]
Al-G1	10	-	70	0.38	Wrinkled sheets
Al-G2	15	-	120	0.38	High amount of wrinkled sheets
Al-GC1	25	33	139	0.39	Wrinkled sheets and small amount of spherical particles
Al-GC2	35	57	145	0.53	Small amount of wrinkled sheets and high amount of spherical particles
*Al-C	25	100	180	0.56	Spherical particles

[a] Error of measurement = ±5%

* Pure χ-Al_2O_3

Table 2 H_2 chemisorption results

Catalyst samples	Amounts of H_2 chemisorption (μmol/g cat.)[a]				% Co dispersion[b]				dp Co^0 (nm) (96.2/D%)			
	5%Co	10%Co	15%Co	20%Co	5%Co	10%Co	15%Co	20%Co	5%Co	10%Co	15%Co	20%Co
Co/Al-G1	0	0.9	9.2	3.3	0	0.1	0.7	0.2	0	962	137	481
Co/Al-G2	0.9	2.3	14.9	10.9	0.2	0.3	1.2	0.6	481	321	80	160
Co/Al-GC1	5.6	7.6	18.9	19.5	1.1	1.1	1.5	1.5	87	87	64	64
Co/Al-GC2	5.8	20.7	21.4	24.6	1.3	1.7	1.7	1.8	74	57	57	53
*Co/Al-C	-	-	16.8	-	-	-	1.3	-	-	-	74	-

[a] Error = ±5 %, as determined directly.

[b] % Co dispersion = [2 ×(total H_2 chemisorption/g cat.) / (no. of μmol of Co total/g cat.)] ×100 %

* Co/Al_2O_3 prepared from pure χAl_2O_3 support.

Table 3 Surface compositions based on XPS results for 15 wt% Co/Al_2O_3 catalysts

Sample	Binding Energy (eV)			Atomic Concentration (%)	
	Co 2p	O 1s	Al 2s	Al/O	Co/Al
15Co/Al-G1	782.4	533.1	120.9	0.29	0.026
15Co/Al-G2	782.4	533.1	120.6	0.33	0.027
15Co/Al-GC1	782.8	533.1	121.0	0.34	0.015
15Co/Al-GC2	782.9	532.9	120.3	0.40	0.019

Table 4 Reaction rate for CO hydrogenation on Co/Al_2O_3 catalysts.

Catalyst samples	CO conversion (%)[a]				Rate (μmol $gcat^{-1}s^{-1}$)[b]				TOF (s^{-1})[b,c]			
	5%Co	10%Co	15%Co	20%Co	5%Co	10%Co	15%Co	20%Co	5%Co	10%Co	15%Co	20%Co
Co/Al-G1	0.5	1.9	8.8	2.1	0.3	1.1	5.2	1.3	-	0.6	0.3	0.2
Co/Al-G2	1.1	2.6	10.0	4.0	0.7	1.6	6.0	2.4	0.4	0.3	0.2	0.1
Co/Al-GC1	2.9	5.5	10.2	7.3	1.7	3.3	6.1	4.3	0.2	0.2	0.2	0.1
Co/Al-GC2	4.0	8.5	10.6	10.7	2.4	5.1	6.3	6.3	0.2	0.1	0.1	0.2

[a] CO hydrogenation was carried out at 220°C, 1 atm, and $H_2/CO/Ar$ = 80/8/32.

[b] Error of measurement = ±5% as determined directly.

[c] Based on H_2 chemisorption.

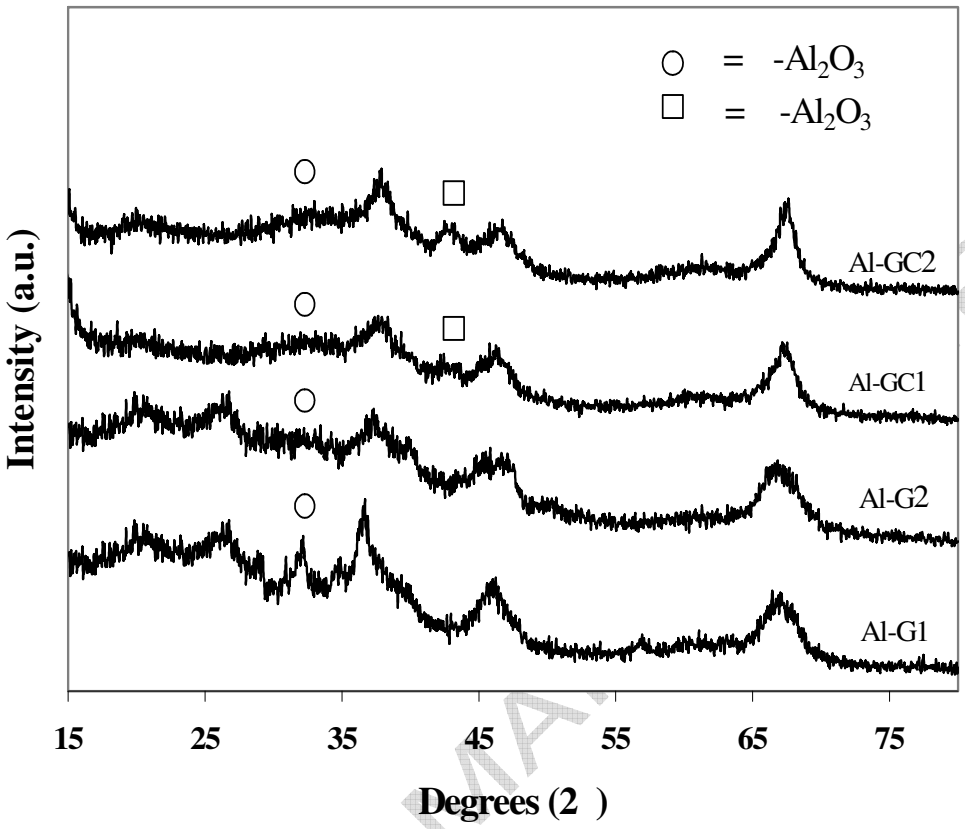

Figure 1 XRD patterns of the various nanocrystalline alumina prepared by the reaction of AIP in 1-butanol at 300°C for 2 h (after calcination at 600°C for 1 h).

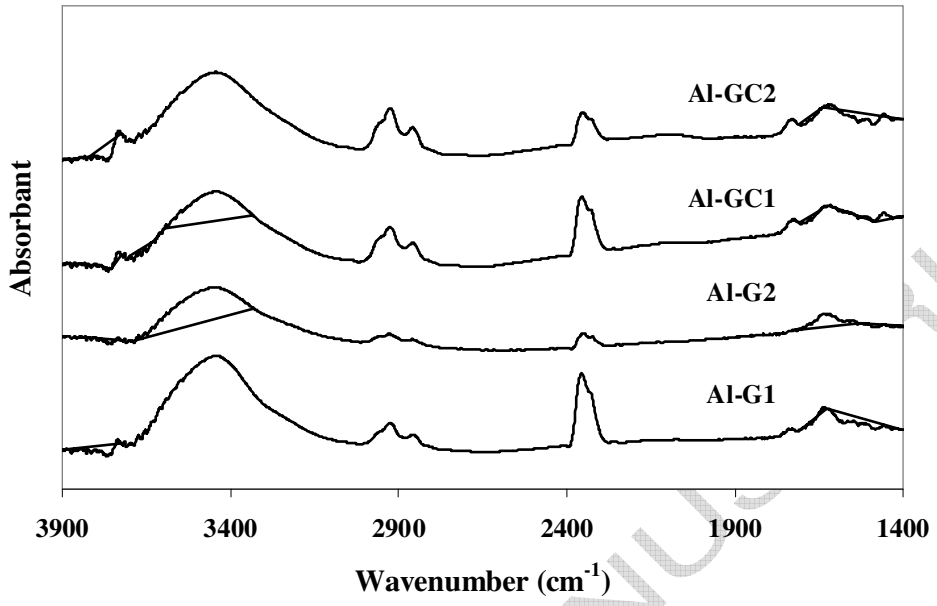

Figure 2 IR spectra of various alumina supports.

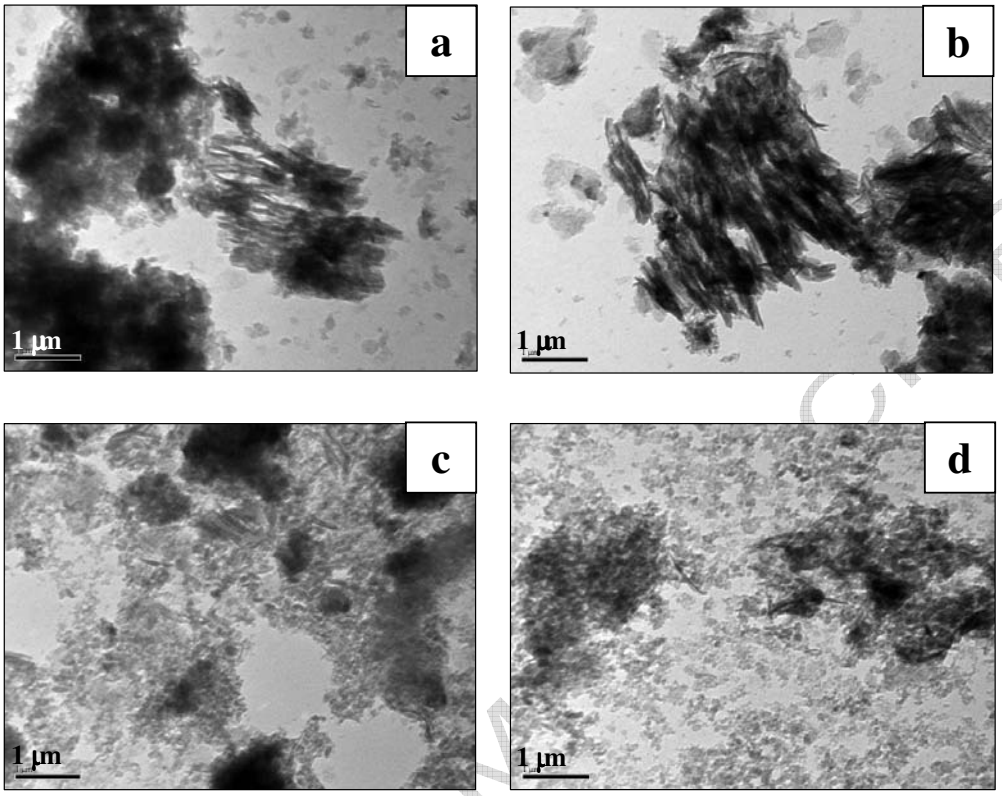

Figure 3 TEM micrographs of the various 20 wt% Co/Al_2O_3 catalysts

(a) 20Co/Al-G1 (b) 20Co/Al-G2 (c) 20Co/Al-GC1 (d) 20Co/Al-GC2.

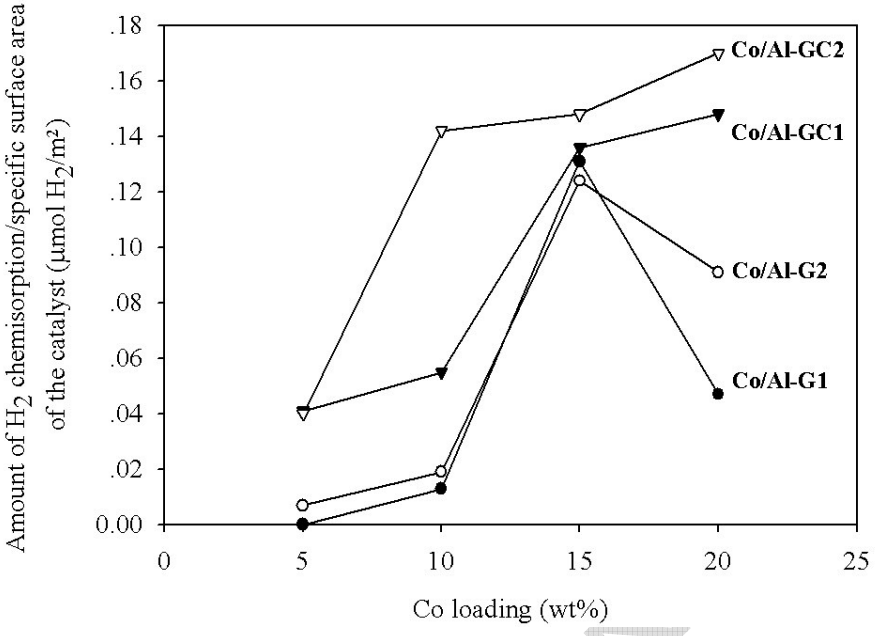

Figure 4 The amount of H_2 chemisorption/specific surface area of the Co/Al_2O_3 catalysts as a function of cobalt loading.

References

[1] R. J. Farrauto, C. H. Bartholomew, Fundamentals of Industrial Catalytic Processes, (Blackie Academic & Professional, London, 1997).

[2] K. V. R. Chary, G. Kishan, C. P. Kumar, G. V. Sagar, Appl. Catal. A 246 (2003) 335.

[3] A. Esteban-Cubillo, C. Diaz, A. Fernandez, L. A. Diaz, C. Pecharroman, R. Torrcillas, J. S. Moya, J. European Ceramic Soc. 26 (2006) 1-7

[4] M. Inoue, H. Kominami, T. Inui, J. Am. Ceram. Soc. 73 (1990) 1100.

[5] M. Inoue, H. Kominami, T. Inui, J. Chem. Soc. Dalton Trans. (1991) 3331.

[6] M. Inoue, H. Kominami, T. Inui, J. Am. Ceram. Soc. 75 (1992) 2597.

[7] M. Inoue, H. Kominami, T. Inui, Appl. Catal. A 77 (1993) L25.

[8] M. Inoue, Y. Kondo, T. Inui, Inorg. Chem. 27 (1988) 215.

[9] Y. Deng, X. Zhou, G. Wei, J. Liu, C.W. Nan, S. Zhao, J. Phys. Chem. Solids 63 (2002) 2119.

[10] Y. Deng, G.D. Wei, C.W. Nan, Chem. Phys. Lett. 368 (2003) 639.

[11] O. Mekasuwandumrong, P. L. Silveston, P. Praserthdam, M. Inoue, V. Pavarajarn, W. Tanakulrungsank, Inorg. Chem. Commun. 6 (2003) 930.

[12] R. C. Reuel, C. H. Bartholomew, J. Catal. 85 (1984) 63.

[13] M. Inoue, H. Otsu, H. Kominami, T. Inui, Ind. Eng. Chem. Res. 35 (1995) 295.

[14] P. Praserthdam, M. Inoue, O. Mekasuvandumrong, W. Tanakulrungsank, S. Phatanasri, Inorg. Chem. Commun. 3 (2000) 671.

[15] J.B. Peri, J. Phys. Chem. 69 (1965) 211.

[16] B. Jongsomjit, T. Wongsalee, P. Praserthdam, Mater. Chem. Phys. 92 (2005) 572.

[17] L. B. Backman, A. Rautiainen, A. O. I. Krause, M. Lindblad, Catal. Today 43

(1998) 11.

[18] L. B. Backman, A. Rautiainen, M. Lindblad, A. O. I. Krause, Appl. Catal. A 191 (2000) 55.

[19] G. Jacobs, T. K. Das, Y. Zhang, J. Li, G. Racoillet, B. H. Davis, Appl. Catal. A 223 (2002) 263.

[20] A. Martinez, C. Lopez, F. Marquez, I. Diaz, J. Catal. 220 (2003) 486.

[21] S. A. Hosseini, A. Taeb, F. Feyzi, Catal. Commun. 6 (2005) 233.

[22] V. Ragaini, R. Carli, C. L. Bianchi, D. Lorenzetti, G. Predieri, P. Moggi, Appl. Catal. A 139 (1996) 31.

[23] J. Panpranot, J. G. Goodwin, Jr., and A. Sayari, Catal. Today 77 (2002) 269.

[24] B. G. Johnson, C. H. Bartholomew, D. W. Goodman, J. Catal. 128 (1991) 231.

[25] E. Iglesia, Appl. Catal. A 161 (1997) 59.

[26] N. Tsubaki, S. Sun, K. Fujimoto, J. Catal. 199 (2001) 236.

[27] K. Pansanga, O. Mekasuwandumrong, J. Panpranot, P. Praserthdam, Korean J. Chem. Eng., In Press, Corrected Proof.